Proceedings of the 21st ICSMGE, Vienna, Austria, 14 – 19 June 2026. Pistrol, Adam & Schweiger (eds.)
Published by: ÖGG, Austrian Society for Geomechanics, Salzburg, Austria, ISBN 978-3-9503898-4-5
https://doi.org/10.53243/ICSMGE2026-361

Investigating the risk of brittle behaviour in collapsible soils beneath a tailings storage facility: A case study

Massyn Harmse, Nico Vermeulen, Rudi Aschenborn
Geotechnical Engineering, Jones & Wagener, South Africa, harmse@jaws.co.za

ABSTRACT: Understanding the risks that natural foundation soils pose to the stability of tailings storage facilities (TSFs) is crucial for ensuring their safe operation and closure. In South Africa, collapsible soils have long been considered problems, particularly in the context of foundation design. However, their potential for brittle, strain-softening response under undrained loading – triggered by the collapse of the metastable arrangement of particles - requires further investigation. This case study investigates a layer of collapsible soil beneath a TSF, focussing on the processes followed to assess its susceptibility to brittle strength loss. An advanced laboratory testing campaign was undertaken to specifically investigate this concern. The results indicate that, although the soil exhibits collapse potential in its natural state, the loading imposed during raising of the TSF embankment reduces the likelihood of brittle, strain-softening behaviour. This mitigation is progressive: as the embankment load increases, the collapsible foundation soils become increasingly densified. These findings underscore the importance of site-specific geotechnical investigations in evaluating and mitigating risks to TSF stability, particularly in the presence of collapsible soils..

KEYWORDS: Collapse potential, liquefaction, brittleness, undrained strength, stability

1 INTRODUCTION

It was initially thought that collapsible soils only occur in loose, aeolian deposits in South Africa. This, however, changed in 1957 during a geotechnical investigation into the differential settlement of a water tower near White River. This was the first reported case of collapse settlement of a residual granite soil of the Basement Complex (Schwartz, 1985). Since then, collapse settlement potential has been identified in a range of transported and residual soils. Schwartz (1985) indicated that problems with collapsible grain structure are encountered in the majority of transported soils which include hillwash, gulleywash, aeolian and littoral deposits and that residual granitic soils of the Basement Complex are generally collapsible. Extensive foundation problems within the Johannesburg–Pretoria granite inlier demonstrate that residual soils derived from the Basement Complex granite present significant design challenges due to their collapsible nature.

Although the impact of collapsible soils on foundations and foundation design is well understood in South Africa, and probably the rest of the world, the impact that a collapsible soil could have on the stability of a TSF is relatively unknown. Key concerns include collapse settlement, which may lead to uniform or differential movements and a consequent reduction in freeboard. These are deformation-related effects resulting from the compression of collapsible soils. An additional concern is the potential for the collapsible horizon to undergo static liquefaction and/or brittle strength loss upon triggering. In such a scenario, the foundation layer could act as a weak layer, commonly referred to as a "banana peel", potentially compromising the stability of the TSF embankment and resulting in a breach or loss-of-containment failure.

This paper presents a case study evaluating the potential for brittle strength loss in a collapsible hillwash foundation horizon beneath an active TSF. The aim is to demonstrate a practical approach for assessing strain-softening risks.

2 LITERATURE REVIEW

2.1 *Collapse potential*

Rogers (1995) defined collapsible soils as a soil of which the soil grains have a metastable, open packing that can undergo collapse. Upon collapse, the open grain structure becomes closer packed, resulting in a significantly reduced volume and more stable grain structure. Collapsible soils are typically characterised by:

- An open grain structure (meta-stable)
- A high void ratio (low dry density & high porosity)
- Geologically young or recently altered deposit
- High sensitivity
- Low or no interparticle bond strength

The most commonly used test method to quantify collapse potential is the collapse potential oedometer test proposed by Jennings & Knight (1975). The authors emphasized that this test yields the Collapse Potential as a percentage volume change (Δe), but that it is not a design parameter as such.

The test is performed on a specimen of soil cut from an undisturbed sample. The specimen is placed into an oedometer ring at its in-situ moisture content. The sample is then loaded to 200 kPa vertical effective stress whereafter it is inundated with water. After 24 hours, the oedometer test is continued in the usual way to the final load specified.

The Collapse Potential is defined as follows:

$$Collapse\ Potential\ (\%) = \frac{\Delta e_c}{1 + e_0}\ x\ 100 \qquad (1)$$

Where Δe_c is defined as the change in void ratio during saturation at 200 kPa and e_0 as the initial void ratio.

2.2 *Brittleness and liquefaction*

The concept of brittleness of soils was first proposed by Bishop (1967, 1973) following the failure of the Aberfan coal tip in Whales on 21 October 1966. Bishop referred to brittleness as the post-peak loss of strength (drained or undrained) of soils under continued shear, and defined the Brittleness Index (I_B) as follows:

$$I_{B(DRAINED)} = \frac{\tau_{peak} - \tau_{residual}}{\tau_{peak}}\ x\ 100 \qquad (2)$$

$$I_{B(UNDRAINED)} = \frac{s_{u(peak)} - s_{u(residual)}}{s_{u(peak)}}\ x\ 100 \qquad (3)$$

Where:

$\tau_{(peak)}$ = Peak drained shear strength (kPa)

$\tau_{(residual)}$ = Residual drained shear strength (kPa)

$s_{u(peak)}$ = Peak undrained shear strength (kPa)

$s_{u(residual)}$ = Residual undrained shear strength (kPa)

As described by Jefferies & Been (2016), soil liquefaction occurs when a soil loses the majority of its strength or stiffness. The idea that static liquefaction was due to considerable brittle strength reduction gave rise to the view that liquefaction occurs due to the collapse of a metastable arrangement of soil particles in a liquefiable soil. In the case of a collapsible soil, this makes sense seeing that the fragile arrangement of particles could collapse upon triggering.

Jefferies and Been (2016) clarify that brittleness, or strength loss, can result from any form of strain-softening behaviour, not solely from grain structure collapse. In general terms, brittleness depends on the relationship between stress state and density state that leads either to contraction of the soil skeleton under drained conditions or to the generation of positive excess pore pressures under undrained conditions under strain, both of which are associated with a loss in strength.

The loss of strength is best illustrated by the stress path in mean normal effective stress (p') and deviator stress (q') space for a Consolidated Undrained (CU) triaxial test. For a soil that does not exhibit strain softening behaviour, the specimen will contract (curve to the left of the initial stress, p'_0) and fail at the critical state line (CSL) at a peak q'. When considering Figure 1 (Atkinson & Bransby, 1978), a normally consolidated, non-strain softening soil follows undrained stress path DBE with failure at E (peak q').

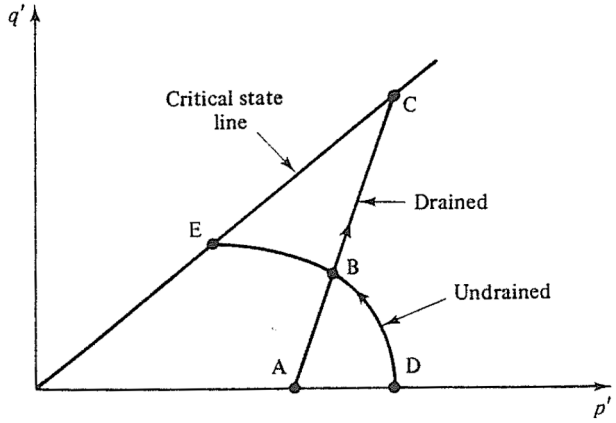

Figure 1. Drained and undrained stress paths in p':q' space.

Figure 2 presents an undrained stress path ABC for a soil that exhibits strain softening behaviour. The specimen achieved peak q' at B whereafter strain softening took place. Unlike the undrained stress path in Figure 1, failure now takes place at C at a lower q' than the peak q' achieved at B.

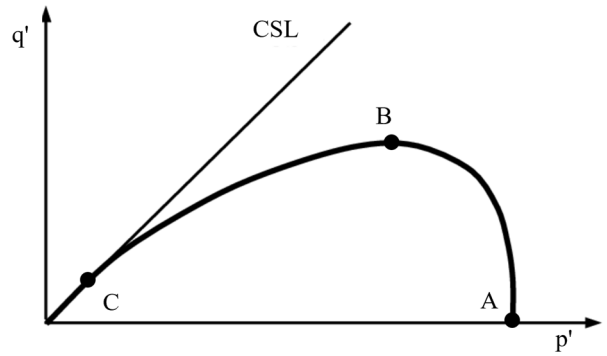

Figure 2. Strain softening stress path in p':'q space.

3 TSF INTRODUCTION

3.1 *Site locality*

This case study is based on a TSF located in South Africa. To maintain confidentiality, no reference is made to the mine, its location, or any identifying details of the TSF.

3.2 *Construction methodology*

The TSF was originally constructed as an upstream, self-raised facility and consists of two compartments. Compartment A was constructed about 10 years before the construction of Compartment B. Compartment A was in operation for about 20 years and Compartment B for about 10 years before both were converted to full containment facilities by means of a waste rock impoundment wall. The construction of the waste rock impoundment wall is ongoing, and both compartments are still in operation.

3.3 *Regional geology*

The geology underlying the TSF is very complex. In general, the site is underlain by quartzofeldspathic gneisses to metasediments. Outliers of Karoo rocks are also present in the area.

3.4 *Shallow subsurface profile*

A geotechnical investigation was carried out in the early 2000's. This investigation found that the general soil profile comprises a loose to medium dense silty sand with a small, variable nodular calcrete and gravel fraction, ranging from 0.5 m to 2.5 m in thickness. The origin was interpreted as transported soil of mixed origin, i.e. aeolian sand overlying hillwash. The investigation concluded that the windblown sands in the upper 0.5 m to 1.0 m of the profile exhibit a potentially collapsible grain fabric. No risk of collapse deformation was envisaged at the time due to the extensive calcrete pedogenesis in the profile and a medium dense or better consistency.

Another investigation was carried out in the 2010's. This investigation yielded two soil profiles, namely:

- Profile A: Shallow bedrock profile.
- Profile B: Thick hillwash sand profile.

Profile A is present below most of the proposed facility and comprises a variable thickness (0.2 m to 0.6 m) of topsoil and a colluvial gravel in a silty sand matrix. Locally, the colluvial gravel is up to 1.2 m thick. The transported soils are often underlain by very stiff, finely laminated micaceous residual silt to depths of 2.5 m. The rock head is typically weathered and soft rock to hard rock in consistency, ranging from quartzites, granite gneisses to biotite gneiss amphibolites and calc-silicate rocks.

Profile B was encountered in the north-western section of the facility. The profile is characterised by thick, silty, coarse and medium sand with calcrete nodules. The material typically extended to the reach depth of a TLB (3.0 m). Below a depth of approximately 1.6 m, closely packed calcrete nodules and gravels are encountered. Most notably, the hillwash is pinhole voided in its natural state.

More recently, in the 2020's, another geotechnical investigation was carried out along the perimeter of the TSF.

3.5 *In-situ Testing*

During the most recent investigation, a Seismic Cone Penetration (SPCTu) test campaign was carried out with the intention of probing into the soils underlying the TSF.

Unfortunately, the SCPTu tests refused in the tailings or the original starter wall prior to reaching the hillwash horizon.

One test did manage to penetrate slightly into the hillwash prior to refusal, but the result was inconclusive regarding the in-situ state and expected behaviour of the hillwash.

3.6 *Laboratory testing*

3.6.1 *Classification testing*

The hillwash comprises about 60% sand sized particles and has a fines content of 35% (silty and clay sized particles). The hillwash is medium plastic with a Plasticity Index (PI) of 15% on average and classifies as a clayey sand (SC) according to the Unified Soil Classification System (USCS).

3.6.2 *Collapse potential*

Collapse potential testing was carried out on the hillwash (Profile B) sampled as part of the second geotechnical investigation. The samples were taken from the toe of the facility and were, therefore, not representative of the state of the hillwash below the TSF embankment.

Collapse potential tests at 100 kPa (not 200 kPa as per the recommendations of Jennings and Knight, 1975) yielded between 9% and 14% collapse potential.

Samples, again taken from the toe of the TSF, during the most recent geotechnical investigation were subjected to the standard collapse potential tests (200 kPa). Similar results were obtained with a collapse potential between 9% and 15%.

3.6.3 *Brittleness*

In addition to the collapse potential tests mentioned above, provision was also made for CU triaxial testing as part of the most recent investigations.

During the sample preparation phase, carving the undisturbed block samples to the required size for a conventional CU triaxial test (50 mm diameter by 100 mm high) proved to be a challenge. Due to the presence of calcrete nodules and quartz gravels, irregular breakage was a common occurrence. Due to this, only one specimen could be carved and tested successfully.

A CU triaxial test was performed on this specimen. The specimen was isotropically consolidated to a mean effective stress (p') of 1 MPa before undrained shearing. Figure 3 presents the stress path in p':q' space.

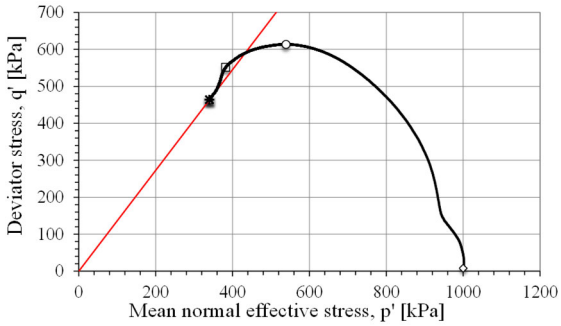

Figure 3. Stress path in p':q' space.

Using the triaxial data, brittleness (I_B) was assessed by plotting the normalised shear stress (q'/q'_{max}) against axial strain, refer Figure 4. The following ranges and descriptions are recommended as per ICOLD Bulletin 194 (2022):

- $I_B < 0.2$ Generally Non-Brittle
- $0.2 < I_B < 0.4$ Slightly Brittle
- $I_B > 0.4$ Highly Brittle

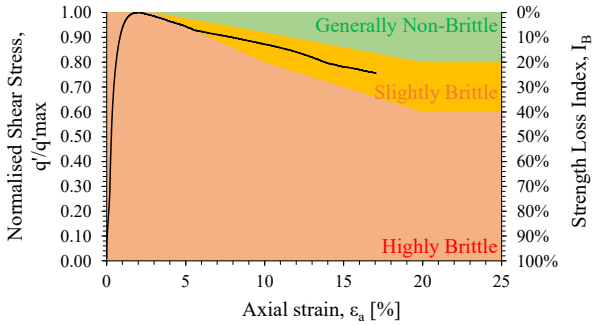

Figure 4. Brittleness during undrained loading.

Based on the stress path in Figure 3, it can be seen that some strength loss took place close to or at the CSL. Upon closer inspection of the post-test condition of the specimen, it was noted that the top cap tilted severely. Hence, the post peak results are questionable as the loss of strength could be attributed to loss of integrity of the external measurements due to tilting of the top cap.

According to Figure 4 the hillwash would classify as slightly brittle. However, there were doubts as to whether the brittleness was due to actually strength loss or an artefact of the test data.

This necessitated a further investigation, specifically designed to mitigate the challenges faced during sampling, specimen preparation and testing.

4 INVESTIGATION METHODOLOGY

4.1 *Background*

Based on the laboratory testing presented in the preceding section, the hillwash is potentially collapsible and brittle, and may be susceptible to strain-softening related strength loss. A further consideration is whether the hillwash has retained its collapsible grain fabric and brittleness potential following construction of the waste rock impoundment wall, given the overburden stress imposed by the wall.

The waste rock impoundment wall has a benched configuration with the crest being 60 m high at its highest section. Assuming a unit weight of 20 kN/m^3, the overburden stress at the base of the highest section of the waste rock wall equals 1200 kPa. It is plausible that at such a high overburden stress, the hillwash could have densified to the extent that mechanical collapse and contractive brittleness are no longer a concern.

In addition, the TSF is unlined and hence, it remains unclear whether seepage from the TSF may have infiltrated the hillwash horizon and triggered collapse. If this is the case, the collapsible grain structure would have been destroyed, regardless of the overburden stress. For the purposes of this case study, the latter was not investigated further.

To confirm the above, an additional sampling and laboratory testing campaign was commissioned, as discussed in the sections to follow.

4.2 *Purpose*

Significant challenges were encountered when preparing 50 mm diameter triaxial test specimens from the original block samples. The specimens frequently broke or developed large voids along the sides where gravel particles were dislodged. To address these issues, it was decided to conduct large-diameter consolidated undrained (CU) triaxial tests using specimens 150 mm in diameter and 300 mm in height. It was postulated that gravel breakout or specimen breakage would be less of a problem for the larger samples.

4.3 *Sampling methodology*

4.3.1 *Equipment*

During the previous campaigns, block samples were carved from the side wall of test pits using a geological pick and other hand tools. It took considerable time and effort to isolate an appropriately large intact block of soil. Even then, the sample would often break apart before it could be successfully wrapped and crated for transportation.

Given the fact that the hillwash is quite competent in its dry desiccated natural state, sampling by means of a concrete core drill was selected:

- A variety of core barrel diameters are available, allowing the option to core samples that are large enough for the large diameter triaxial tests. A 154 mm diameter core barrel was used in this case.
- The cutting edge can cut through quartz gravels and calcrete nodules if the barrel is advanced slow enough. Hence, reducing the risk of breakage or fall out.
- Seeing that the sample can be cored to the correct diameter, the need for further specimen trimming is reduced, hence reducing the risk of breakage when preparing the test specimens.

4.3.2 *Sampling*

Sampling was conducted over a period of three days. Initially, the topsoil was removed using an excavator to expose the top of the hillwash horizon. The exposed surface was then levelled with hand tools prior to setting up the core drill.

Coring commenced from the top of the cleared area. It was observed early in the process that cuttings were becoming lodged in the barrel, leading to sample disturbance and damage. To resolve this issue, a trench was excavated through the centre of the cleared area, adjacent to the sampling position. An opening was then created from the trench sidewall to the cutting edge of the advancing barrel, allowing cuttings to evacuate freely and reduce sample disturbance.

A total of eight samples were cored. The samples were wrapped in clingfilm and tinfoil prior to being placed into a PVC split mould. The split mould was slightly larger than the sample, hence the annulus was filled with expanding foam. All eight samples were transported in a specially designed, foam lined crate to the laboratory.

Figure 5 shows the coring process in progress. The cuttings evacuation channel can be seen to the left of the barrel. Figure 6 shows a core sample after it was extracted from the core barrel. Although this method of sampling worked well, some imperfections are visible on the surface of the sample. This varied between the various samples retrieved.

Figure 5. Sample coring on site.

Figure 6. Extracted core sample prior to packaging.

4.4 *Laboratory test campaign*

The laboratory test campaign included carrying out large diameter CU triaxial tests on the undisturbed hillwash core samples. A total of eight samples were submitted to the laboratory in case some samples sustained damage during transport.

The purpose of the test campaign was to:

- Establish whether the loading from the waste rock impoundment wall is sufficient to densify the hillwash to the extent that the collapsible grain structure is destroyed, and to
- Determine the I_B of the hillwash specimens at the various load conditions.

In theory, it is expected that the hillwash horizon outside the footprint of the TSF is normally consolidated. Hence, the hillwash would exhibit contractive behaviour under undrained shearing. However, the question remained whether the specimen is sufficiently loose to exhibit brittle strain softening behaviour. It was postulated that at high p', the specimen would densify to the extent that a brittle strain softening response is no longer possible. The specimen would still yield a contractive response, but brittle strength loss would have been mitigated.

The test specifications were as follows:

- Dry consolidation of four specimens to 100 kPa, 200 kPa, 400 kPa and 1 200 kPa total stress. The flushing and saturation phases were deliberately delayed until the desired consolidation stress was achieved to not induce collapse through wetting.
- Once the desired consolidation stress was reached, the specimens were flushed and saturated.
- Once saturation was completed, the specimens were subjected to undrained shearing to 25% axial strain.

For comparison, an additional specimen was tested using the conventional CU triaxial procedure whereby flushing and saturation is conducted prior to the consolidation stage. This specimen was consolidated to a mean effective stress of 1 200 kPa followed by undrained shearing.

To quantify the collapse that occurred during the dry consolidation stages, the consolidated specimen dimensions had to be taken manually. At the end of the specified dry consolidation stage, the specimen was unloaded and the triaxial cell disassembled, allowing measurements to be made with the membrane in place. Once measurements were completed, the cell was reassembled, the specimen reloaded to the specified confinement stresses, and then flushed and saturated.

In general, the testing was considered a success. Close collaboration between the engineers and the laboratory proved to be the main key to achieving the desired outcomes.

The geostatic stress ratio (K_0) and the impact of possible cementation (calcretisation) was unknown at the time of testing. K_0 consolidation could result in brittle response due to principal stress rotation, and the concern was that this could mask structural brittleness or collapse potential. For the purposes of this study, isotropic consolidation was preferred to isolate and focus on structural brittleness.

4.5 *Results discussion*

The results of the large diameter CU triaxial tests in terms of specimen behaviour in p':q' space, brittleness and undrained strengths are presented below.

4.5.1 *Stress paths*

Figure 7 presents a comparison of the four (dry consolidated) plus one (wet consolidated in blue) stress paths for the various specimens in p':q' space.

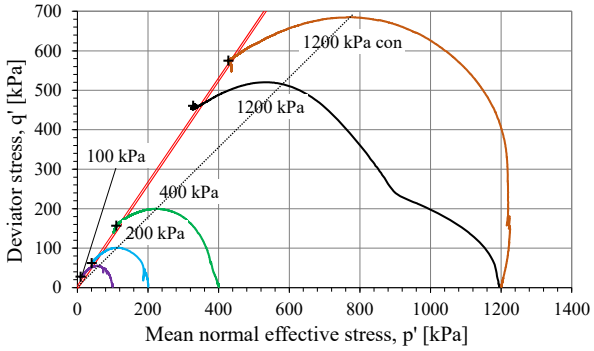

Figure 7. Stress paths in p':q' space.

The hillwash specimens yielded contractive behaviour, regardless of the applied consolidation stress.

All specimens yielded strain softening behaviour as peak q' was achieved prior to strain softening taking place, resulting in failure at the CSL at a lower q'. Interestingly, when a line is drawn through the peak q' for all specimens, the Instability Locus (IL) can be defined (black dashed line). A specimen sheared in undrained conditions may become unstable once the stress path crosses the IL. In the case of the hillwash specimens, the specimens reached the IL and underwent softening, failing at the CSL after strength loss.

The stress paths suggest that the strength loss (difference between peak q' and q' at failure) reduces with increasing confinement stress (p'), thereby reducing the brittleness of the material.

4.5.2 *Brittleness*

Figure 8 presents the normalized shear stress vs axial strain plot for the various specimens.

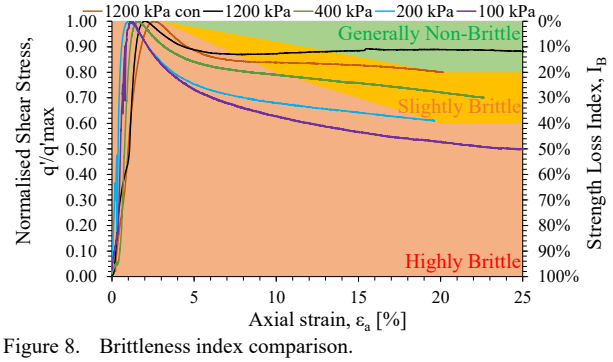

Figure 8. Brittleness index comparison.

The 100 kPa specimen is classified as highly brittle (I_B > 40%). The 200 kPa and 400 kPa specimens exhibit slight brittleness (20% < I_B < 40%). Both 1200 kPa specimens fall within the generally non-brittle range (I_B < 20%), although the dry-consolidated specimen (black) is considered borderline between non-brittle and slightly brittle.

From Figure 8, it can be concluded that the I_B reduces with an increase in p', hence an increase in overburden stress tends to reduce the propensity to brittle strength loss.

4.5.3 *Undrained strength*

Figure 9 presents the Undrained Shear Strength Ratio (USR) vs p' plot for the various specimens. Both the peak USR (PUSR) and residual USR (RUSR) were determined for all specimens based on the CU triaxial results. Note that the open symbols depict the results for the conventionally flushed and saturated CU triaxial consolidated to 1200 kPa (in black).

The PUSR slightly reduces from 0.27 at 100 kPa to 0.22 at 1200 kPa for the dry consolidated specimens. The conventionally flushed and saturated specimen yielded a PUSR of 0.29 at 1200kPa.

The RUSR increases from 0.14 at 100 kPa to about 0.20 at 400 kPa and 1200 kPa, respectively. Again, the conventional CU triaxial yielded a higher RUSR of 0.24.

In general, the PUSR and RUSR tend to converge at higher p' (> 1200 kPa). Hence, the brittleness (difference between PUSR and RUSR) decreases and will likely ultimately converge to a single PUSR at a high enough overburden stress.

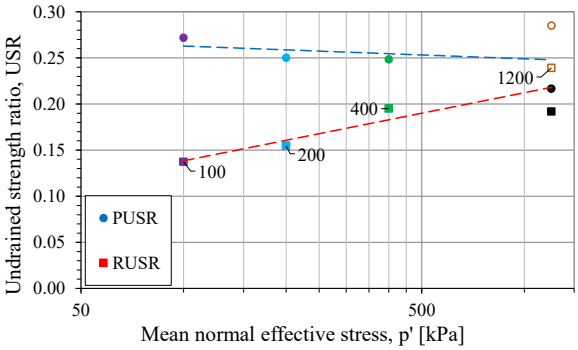

Figure 9. Peak and residual undrained strength comparison.

The results confirm that the hillwash horizon underlying the TSF is capable of sufficient densification under higher overburden stresses to mitigate the risk of brittle, strain-softening behaviour. However, this risk appears to be fully mitigated only at overburden stresses exceeding 1200 kPa.

When considering the conventionally flushed and saturated specimen in isolation, it can be concluded that triggering collapse by wetting at low stress levels does not eliminate the risk of brittle strength loss. Although this specimen was tested at high effective stress (p'), it still exhibited some degree of brittleness. Therefore, assuming that collapse has been triggered, through seepage for example, and that brittleness has consequently been mitigated is not recommended.

5 CONCLUSIONS

This case study investigated the potential brittleness of a natural transported soil (hillwash) with a collapsible fabric. In situ, the collapse potential ranges from 10% to 15%. As this layer now forms part of the foundation beneath a TSF embankment wall, concerns were raised regarding its potential to behave as a weak or unstable foundation stratum.

To address these concerns, a series of investigations was undertaken to quantify the potential for collapse and strain

softening due to brittleness. Large-diameter Consolidated Undrained (CU) triaxial tests confirmed that the hillwash exhibits significant brittleness at low confinement stresses. However, with increasing confinement (surcharge loading from the TSF embankment), the Brittleness Index (I_B) decreases as the residual undrained strength ratio converges to the peak undrained strength ratio. These results demonstrate that the densifying effect of the waste rock impoundment wall progressively suppresses brittle collapse. Nonetheless, the risk was not fully mitigated at the stress levels considered in this study.

The use of 150 mm diameter by 300 mm high core specimens, obtained using a novel low-disturbance coring technique, proved essential for capturing representative behaviour in this gravelly, calcretised soil. The methodology is transferable to similarly challenging materials.

Importantly, laboratory-derived collapse indices alone are insufficient to quantify in-situ brittleness risk. Site-specific, stress-dependent brittleness assessments are therefore recommended where such risks are present. These should include in-situ testing and sampling, preferably from beneath the TSF embankment wall.

This case study bridges the gap between conventional collapse potential assessments and modern concepts of strain-softening behaviour, providing practitioners with a robust basis for evaluating and mitigating brittle failure risks in collapsible foundations worldwide.

6 REFERENCES

Atkinson, J.H. and Bransby, P.L., 1978. The mechanics of soils: an introduction to critical state soil mechanics. London: McGraw-Hill.

Bishop, A.W., 1967. Progressive failure—with special reference to the mechanism causing it. In: Proceedings of the Geotechnical Conference on Shear Strength Properties of Natural Soils and Rocks, Oslo, 1967. Oslo: Norwegian Geotechnical Institute, pp. 142–150.

Bishop, A.W., 1973. The stability of tips and spoil heaps. Quarterly Journal of Engineering Geology and Hydrogeology, 6, pp. 335–376.

Jefferies, M.G. and Been, K., 2016. Soil liquefaction: a critical state approach. 2nd ed., CRC Press/Taylor & Francis, p. 690.

Jennings, J.E. and Knight, K., 1975. A guide to construction on or with materials exhibiting additional settlement due to 'collapse' of grain structure. Proceedings of the 6th Regional Conference for Africa on Soil Mechanics and Foundation Engineering, Durban, South Africa, 1–6 September 1975. Durban: South African Institution of Civil Engineering, pp. 99–105.

International Commission on Large Dams (ICOLD), "Bulletin No. 194: Tailings dam safety," Paris, 2022.

Rogers, C.D.F., 1995. Types and distribution of collapsible soils. In: E. Derbyshire, T. Dijkstra and I.J. Smalley, eds. Genesis and properties of collapsible soils. Dordrecht: Springer (NATO ASI Series C: Mathematical and Physical Sciences, 468), pp. 1–17.

Schwartz, K. (1985). Problem Soils in South Africa - State of the Art: Collapsible Soils. The Civil Engineer in South Africa, Volume 27, No. 7.

U.S. Army Corps of Engineers (USACE) and U.S. Bureau of Reclamation (USBR), 2006. Engineer Manual EM 1110-1-4000: Unified Soil Classification System. Washington, DC: U.S. Department of the Army.